DOI:
10.1111/jcpe.14034

Document Version
Publisher's PDF, also known as Version of record

Received: 16 March 2024 | Revised: 3 May 2024 | Accepted: 10 June 2024

DOI: 10.1111/jcpe.14034

ORIGINAL ARTICLE

Journal of Clinical Periodontology WILEY

Microbiological and molecular profile of furcation defects in a population with untreated periodontitis

Pasquale Santamaria[1] | Yi Jin[1] | Mandeep Ghuman[1] | Saeed Shoaie[1] | David Spratt[2] | Giuseppe Troiano[3] | Luigi Nibali[1]

[1]Periodontology Unit, Centre for Host Microbiome Interactions, Faculty of Dentistry, Oral & Craniofacial Sciences, King's College London, London, UK

[2]Microbial Diseases, Eastman Dental Institute, University College London, London, UK

[3]Department of Clinical and Experimental Medicine, University of Foggia, Foggia, Italy

Correspondence
Luigi Nibali, Periodontology Unit, Centre for Host Microbiome Interactions, Faculty of Dentistry, Oral & Craniofacial Sciences, King's College London, Floor 17, Guy's Tower, Guy's Hospital, Great Maze Pond, London SE1 1UL, UK.
Email: luigi.nibali@kcl.ac.uk

Abstract

Aim: To describe the microbiological composition of subgingival dental plaque and molecular profile of gingival crevicular fluid (GCF) of periodontal furcation-involved defects.

Materials and Methods: Fifty-seven participants with periodontitis contributed with a degree II–III furcation involvement (FI), a non-furcation (NF) periodontal defect and a periodontally healthy site (HS). Subgingival plaque was analysed by sequencing the V3–V4 region of the 16S rRNA gene, and a multiplex bead immunoassay was carried out to estimate the GCF levels of 18 GCF biomarkers. Aiming to explore inherent patterns and the intrinsic structure of data, an AI-clustering method was also applied.

Results: In total, 171 subgingival plaque and 84 GCF samples were analysed. Four microbiome clusters were identified and associated with FI, NF and HS. A reduced aerobic microbiota ($p = .01$) was detected in FI compared with NF; IL-6, MMP-3, MMP-8, BMP-2, SOST, EGF and TIMP-1 levels were increased in the GCF of FI compared with NF.

Conclusions: This is the first study to profile periodontal furcation defects from a microbiological and inflammatory standpoint using conventional and AI-based analyses. A reduced aerobic microbial biofilm and an increase of several inflammatory, connective tissue degradation and repair markers were detected compared with other periodontal defects.

KEYWORDS
dental plaque, gingival crevicular fluid, microbiology, periodontal bone loss, periodontitis

Clinical Relevance

Scientific rationale for study: To profile subgingival microbiological and molecular environment of periodontal furcation defects in patients with untreated periodontitis.

Principal findings: Decrease levels of aerobic taxa and an increase of several molecular biomarkers were detected in the furcation defects compared with other periodontal defects.

Practical implications: The increased risk of tooth loss of furcation defects may be partially explained by the specific microbiological and molecular profile, representing an opportunity to generate new hypotheses to develop a personalized therapeutic approach of furcation sites.

1 | INTRODUCTION

Periodontitis is an inflammatory process that predisposes to perturbation of the subgingival microenvironment with the formation of periodontal pockets, which in turn drives the selection of pathogenic microbiological profiles. The resulting dysbiosis in these periodontal pockets triggers the host-response cascade activation with several bacterial and anti-bacterial cell types, signalling molecules, and inflammatory products detected in the gingival crevicular fluid (GCF) (Pellegrini et al., 2017). Interestingly, the term periodontal pockets is commonly used to define any type of diseased site: vertical, suprabony and furcation involvement (FI). This assumes that FI is simply an extension of periodontal pockets, although direct microbiological and histopathological data are lacking (Al-Shammari et al., 2001; Glickman, 1950). FI represents a unique therapeutic challenge, as it is associated with an increased risk of tooth loss, even when supportive periodontal care (SPC) is carried out (Nibali et al., 2017; Trullenque-Eriksson et al., 2023). Less effective mechanical removal of subgingival plaque in poorly accessible furcation areas results in increased microbial colonization and limited response to periodontal treatment when compared with single-rooted teeth (Gill et al., 2022).

Knowledge of the composition of subgingival biofilm in periodontal furcation defects is sparse. Overall microbiological counts and anaerobic counts have previously been reported to be higher for furcation areas when compared with non-furcation (NF) sites after subgingival debridement (Loos et al., 1988). 16s rRNA analysis of 39 molar furcation areas before surgical treatment found a similar microbiological composition between FI and 'severe' periodontal lesions, but a less 'representative' core microbiome in FI when compared with other periodontal defect types (Queiroz et al., 2017).

Similarly, GCF has been used to study the molecular profile collected in periodontal defects with different anatomical configurations. Interestingly, both infrabony defects and suprabony defects show significantly increased concentrations of inflammatory and connective tissue degradation markers in GCF, as well as markers of repair/regeneration when compared with healthy sites (HS) (Koidou et al., 2022; Santamaria et al., 2023). However, the molecular profile of the GCF markers failed to distinguish between infrabony and suprabony defects.

The effect of furcation involvement on the subgingival microbiome and molecular profile of GCF is unknown. Therefore, the primary aim of this investigation was to conduct a taxonomic analysis of the subgingival microbiota of FI compared with NF and HS in patients with untreated periodontitis. The secondary aims were to identify any molecular difference in GCF among FI, NF and HS, and to develop an AI-validated clustering model to highlight potential microbial interactions among communities found in different periodontal defects.

2 | MATERIALS AND METHODS

2.1 | Study population

Eligible participants involved in King's College London Oral, Dental and Craniofacial Biobank were included in this study (NHS UK Research Ethics Service approval reference 20/EE/0241, provided by the East of England-Cambridge East Research Ethics Committee). Each participant provided written consent to enrol in the Biobank. Approval to access data and samples for the present study was obtained from the Biobank Management Committee (REF007). The STROBE checklist was used to plan the cross-sectional design of the present investigation. The following inclusion criteria were set: (i) age 18–75; (ii) stage III–IV periodontitis (Tonetti et al., 2018); (iii) at least one maxillary or mandibular tooth excluding third molars with: (a) one molar with an FI site with degree II/III horizontal FI (at least between two roots for maxillary molars), class B–C vertical FI (bone loss up to the middle third of root cones), probing pocket depths (PPDs) >5 mm in the furcation area, not readily accessible for self-performed oral hygiene (*test site*); (b) one NF periodontal defect site on a molar with no signs of FI (positive control) (PPD > 4 mm within 1 mm of PPD on test site, radiographic defect depth ≥3 mm); (c) and one periodontally HS (healthy control) (PPD < 4 mm), with no previous signs of radiographic bone loss and no bleeding upon probing. In cases with multiple periodontal defects, sites with deepest PPD were included. In the absence of symmetrical contralateral molars, neighbouring teeth were chosen (in order of other molars, second premolars, first premolars, canines); (iv) mobility < degree II; (v) absence of any ongoing endodontic pathology; (vi) absence of an adjacent tooth with unfavourable periodontal prognosis (as judged by the study clinician). Exclusion criteria were based upon a similar recent study (Santamaria et al., 2023) and included in SupMat 1. Participant recruitment took place between September 2022 and March 2023, with enrolment of 57 consecutive participants fulfilling the aforementioned criteria. Periodontal parameters were measured by the same calibrated examiner (PS) in accordance with our recent study (Santamaria et al., 2023) (SupMat 1), in particular, the furcation classification was done horizontally (Hamp et al., 1975) and vertically (Tarnow & Fletcher, 1984) for FI using a UNC-15 periodontal probe and a Nabers probe. Radiographs were taken according to clinical needs and were used to confirm both the classification of FI and the radiographic defect depth ≥3 mm for the NF.

2.2 | Subgingival plaque sampling

Subgingival plaque samples were collected preferably from the buccal surface of FI sites; alternatively, either mesial or distal furcation sites in maxillary molars, or lingual furcation sites in mandibular molars, were sampled if the buccal furcation was not degree II/III. Before sample collection, the supra-gingival plaque was carefully removed, and the site was isolated with cotton wool rolls and gently dried. A sterile curette was then carefully inserted into the bottom of the pocket and removed with a single stroke, and the content was placed in TE buffer solution (Cat No. 93283 Sigma-Aldrich) and stored at −80°C until the time of analysis.

2.3 | DNA extraction and sequencing

DNA from subgingival plaque samples was extracted following the manufacturer's instructions using the DNeasy PowerSoil Pro Kit

(Qiagen Inc., USA). DNA quantity and quality were assessed spectrophotometrically (Nanodrop 2000C UV–Vis spectrophotometer [Nanodrop Technologies] and a Qubit Fluorometer [Thermo Fisher Scientific, Waltham, Massachusetts, U.S.]). Bacterial 16S rRNA gene region V3–V4 in the samples was amplified using the following primer sequences.

Forward Primer:

5′-TCGTCGGCAGCGTCAGATGTGTATAAGAGACAGCCTACGGGNGGCWGCAG-3′.

Reverse Primer:

5′-GTCTCGTGGGCTCGGAGATGTGTATAAGAGACAGGACTACHVGGGTATCTAATCC-3′.

Amplicons were then barcoded using IDT for Illumina unique dual indexes (UDIs), multiplexed, spiked with 10% *PhiX* and sequenced using the Miseq V3 600 cycle kit in the 300 bp paired-end read method on the Illumina Miseq platform (Illumina, San Diego, CA, USA) at the UCL Genomics Facility, University College of London.

2.4 | Sequence analysis and taxonomic classification

Raw Illumina reads were quality filtered, trimmed, a Q-score >20 for ambiguous bases recovered in the overlapping region and up to two ambiguous bases were allowed in the overlap. Sequences were analysed using the DADA2 1.18 pipeline based on qiime2 platform (qiime2-amplicon-2023.9) to cluster them into amplicon sequence variants (ASVs) and the HOMD V15.1 database to classify each ASV at the genus level. Alpha diversity was analysed with the R package Phyloseq 1.44.0 using the Simpson and Shannon indices as estimators of richness and diversity, respectively. Statistical differences of these estimators based on the variables of the study were assessed using the Kruskal–Wallis test. For beta diversity, principal coordinates analysis (PCoA) of Bray–Curtis dissimilarity was conducted using the Phyloseq package, and differences among the defined groups were assessed using the PERMANOVA test implemented in the adonis function of the vegan 2.6.4 package. Differential abundance of the identified taxa was studied using the Wilcoxon rank-sum test for pairwise comparison and the Kruskal–Wallis test for three groups, filtering the differences by p values smaller than .05, a log2-fold change (L2FC) absolute value higher than 2, and by their base mean value, not considering ASVs with a base mean value pertaining to the lowest quartile. A significance threshold of .05 was used according to previous investigations (Arredondo et al., 2023), with values adjusted by the Bonferroni correction for multiple tests to minimize the overall Type I error rate. The association between the patterns of bacterial genera and the GCF molecular profile was assessed using Pearson correlation, and correlation coefficients greater than .2 or smaller than −.2 were labelled as significant (Seidel et al., 2020). Aerobic, anaerobic and facultative metabolism were also manually assigned to each genus using the Human Oral Microbiome Database (HOMD), and relative percentages per each group were calculated. Statistical analysis was completed using the Kruskal–Wallis test for three groups, filtering the differences by p values smaller than .05.

2.5 | AI-based model for microbiome clustering

16S-rRNA Seq data were then analysed using an autoencoder, which is a type of artificial neural network known for its efficiency in reducing dimensionality while preserving critical information. The autoencoder was designed with variable encoding dimensions, learning rates and activation functions, optimized through a hyperparameter search over specified ranges. The model's architecture included one input layer, multiple hidden layers (based on the number of layers parameter) and an output layer mirroring the input layer's dimensionality. The Adam optimizer and binary cross-entropy loss function were used for training the model. The TensorFlow and Keras libraries facilitated the model's implementation and training. After reduction, the k-means clustering was applied to the reduced features to identify distinct microbial communities within the patient-level adjusted periodontal dataset. The number of clusters was determined through iterative testing, by maximizing some clustering performance metrics: Silhouette score, Davies–Bouldin index and Calinski–Harabasz index, providing insight into cluster cohesion, separation and validity. In particular, a Silhouette score close to 1, a Davies–Bouldin index closer to 0 and a higher Calinski–Harabasz index support a good clustering. Following clustering separation, a random forest classifier was employed to determine the feature importance of microbial genera in distinguishing the identified clusters. The analyses were conducted using Python (version 3.7); a chi-squared test was also conducted to assess the relationship between the site and cluster membership. SupMat 2 includes a detailed protocol of the developed AI-based model.

2.6 | GCF sampling and statistical analysis

GCF collection and analyses of 18 selected GCF markers strictly followed the protocol previously reported (Santamaria et al., 2023) in SupMat 3. GCF volume, PPD and PPD + REC, and the GCF markers between FI (test), NF and HS, concentrations (pg/mL) and total amounts (pg/30s) are described as means and standard deviations (SDs). Non-parametric tests were used for the analysis as GCF markers and volume were not normally distributed. The differences between FI, NF and HS for each of the GCF markers' concentrations were obtained using the independent samples Kruskal–Wallis test. Significance values were adjusted using the Bonferroni correction for multiple tests.

2.7 | Sample size/power calculation

The sample size for the GCF marker analysis was calculated using the VEGF levels of infrabony and HS detected in a previous study (Santamaria et al., 2023). The significance was set at 5% and the power at 90%; therefore, a minimum of 21 patients were required to detect a difference of 200.11 (pg/mL) in IL-1 alpha between FI and HS. For the GCF analysis, 28 participants (three samples each) were included in the investigation to compensate for the multiple GCF

markers and potential lack of markers in some samples. Due to the lack of previous studies, a convenience sample of 57 participants was selected for the plaque analysis to account for potential low DNA quality and/or sample contamination.

3 | RESULTS

Table 1 shows the site-specific periodontal clinical characteristics of the 57 included participants; demographic and general periodontal features are included in SupMat 4.

Overall, 57 (28 GCF) sites were sampled in each group; PPD and PPD + REC were higher in periodontal sites compared with HS ($p < .05$), but there was no significant difference between FI and NF. FI had an average PPD + REC of 7.78 (1.36) mm, while the NF had an average PPD + REC of 7.71 (1.33) mm. HS included 27 contralateral molar, 15 other molars, 10 premolars and 5 canines.

3.1 | Microbiome analysis

3.1.1 | Diversity metrics

Bacterial diversity and richness of the different populations showed significant differences between diseased and HS according to the Shannon and Simpson indices (Figure 1a,b). Higher richness and diversity were observed in FI and NF compared with HS (Shannon $p = 6.0 \times 10^{-4}$, Simpson $p = 3.8 \times 10^{-3}$), although no significant differences were detected between FI and NF defects (Shannon $p = .85$, Simpson $p = .64$). The distribution of the microbial composition was assessed using the PCoA plots of Bray–Curtis (Figure 1c). PCoA ordination analysis showed significant differences in microbial composition for the three groups (FI, NF and HS) (adonis $p = 1.0 \times 10^{-4}$, $R^2 = .081$).

3.1.2 | AI model clustering analysis

The AI model found four distinct microbiome clusters with a Silhouette score of 0.807, a Davies–Bouldin index of 0.406 and a Calinski–Harabasz index of 1626.63, indicating well-defined separate clusters (Figure 2a). The relative percentage of sites showing cluster 0 in FI and NF groups was approximately double (68.42% and 73.68%) when compared with HS (35.09%). On the other hand, for clusters 1 and 2, HS (26.32%, 28.07%) showed a relative percentage more than double that of FI (8.77%, 8.77%) and NF (10.52%, 14.3%). Cluster 3 was more represented by HS (10.53%) and FI (14.4%) compared with NF (1.75%). The 10 most represented ASVs are reported in SupMat3, showing highly predominant periodontal pathogens in cluster 0 compared with clusters 1, 2 and 3.

3.1.3 | Distribution of genera between groups

The overall number of bacterial genera detected in the samples was 152, with 34 genera accounting for slightly more than 50% of the sequences detected in every group site (Figure 2b). *Streptococcus* ($p = 1.7 \times 10^{-4}$), *Rothia* ($p = 9.6 \times 10^{-5}$), *Neisseria* ($p = .002$) and *Lautropia* ($p = 5.8 \times 10^{-7}$) were statistically more represented in HS compared with FI and NF groups. *Selenomonas* ($p = .00053$),

TABLE 1 Periodontal clinical data summarized by site level of included participants.

Site level	PLAQUE			GCF		
	Furcation sites (FI $n = 57$)	Non-furcation sites (NF $n = 57$)	Healthy sites (HS $n = 57$)	Furcation sites (FI $n = 28$)	Non-furcation sites (NF $n = 28$)	Healthy sites (HS $n = 28$)
Average PPD	6.54 (1.11)	6.70 (1.19)	2.35 (0.47)*	6.46 (1.02)	6.46 (1.17)	2.48 (0.58)*
Average PPD + REC	7.78 (1.36)	7.71 (1.33)	2.71 (0.89)*	7.77 (1.47)	7.50 (1.41)	2.89 (0.75)*
Average REC	1.24 (0.97)	1.01 (1.02)	0.36 (0.23)*	1.31 (1.01)	1.04 (1.03)	0.41 (0.51)*
BOP (+:−)	57:0	57:0	0:57	28:0	28:0	0:28
GCF volume (μL)				0.75 (0.32)	0.61 (0.26)	0.33 (0.26)*
Mobility Degree 1 (yes: no)	18:39	10:47	2:55	8:20	5:23	1:28
Horizontal furcation involvement II:III	34:23			15:13		
Vertical furcation involvement B:C	38:19			12:16		
Furcation molars						
Maxillary:Mandibular	37:20			18:10		
First:Second	31:26			20:8		

Note: All data are reported as means (standard deviations). * indicates statistical significance difference between site ($p < .05$).
Abbreviations: BOP, bleeding upon probing; GCF, gingival crevicular fluid; GR, gingival recession; PPD + REC, clinical attachment level; PPD, probing depth.

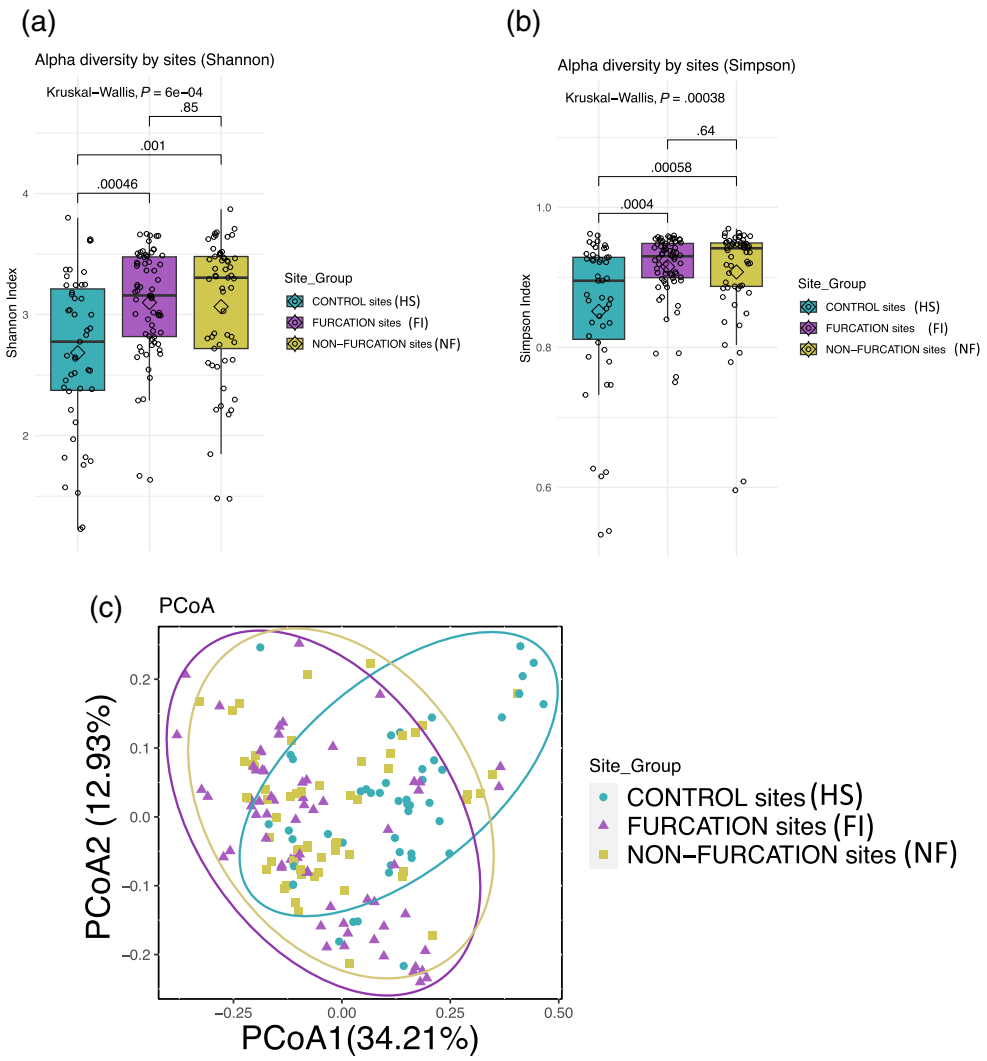

FIGURE 1 Alpha diversity with Shannon index (a) and Simpson index (b) of the microbiota grouped by furcation sites, non-furcation and healthy sites. (c) Principal coordinates analysis of Bray–Curtis of the microbiome structure of the subgingival samples, grouped by furcation sites, non-furcation and healthy sites.

Treponema ($p = 2.2 \times 10^{-4}$), *TG5* ($p = 7.9 \times 10^{-5}$), *Tannerella* ($p = 4.1 \times 10^{-5}$) and *Fusobacterium* ($p = 3.1 \times 10^{-5}$) were more abundant in periodontal defects (FI + NF). Overall, seven genera showed statistical differences between FI and NF (Figure 3). *Neisseria* ($p = .002$), *Fusobacterium* ($p = .032$) and *Cardiobacterium* ($p = .009$) were higher in NF sites than in FI sites, while *Olsenella* ($p = .008$), *Atopobium* ($p = .04$), *Actinomyces* ($p = .002$) and *Moryella* ($p = .02$) were significantly higher in FI than in NF.

3.1.4 | Aerobic metabolism distribution between groups

Each genus detected was also classified according to aerobic, anaerobic and facultative metabolism (Figure 4a–c). The relative percentages in each group (FI, NF, HS) were then calculated, resulting in a higher level of facultative ASVs in the HS compared with NF sites ($p = .0022$), with no significant difference between NF and FI ($p = .08$). For the anaerobic subgroup, significant higher levels were detected in both FI and NF ($p = 2.2 \times 10^{-5}$, $p = 7.4 \times 10^{-6}$) when compared with HS. For the aerobic genera, both FI and NF showed significantly lower levels when compared with HS ($p = 5.9 \times 10^{-6}$, $p = 2.2 \times 10^{-5}$), and FI group showed an even lower level when compared with NF ($p = .0018$).

3.2 | GCF volumes at sampled sites

The GCF volume was similar between FI and NF with no statistical difference, but both types of periodontal defects showed a significantly higher GCF volume compared with HS. (FI mean: 0.75 [0.32]μL, NF mean 0.61 [0.26]μL, HS 0.33 [0.26]μL, [$p = .0001$]) (Table 1).

3.3 | GCF biomarker levels

All 18 markers included in the Luminex analysis were detectable within the range of the immunoassays (Table 2). When comparing HS ($n = 28$) with periodontal defects (FI + NF, $n = 56$), periodontal defects exhibited statistically significant higher ($p < .05$) GCF levels of

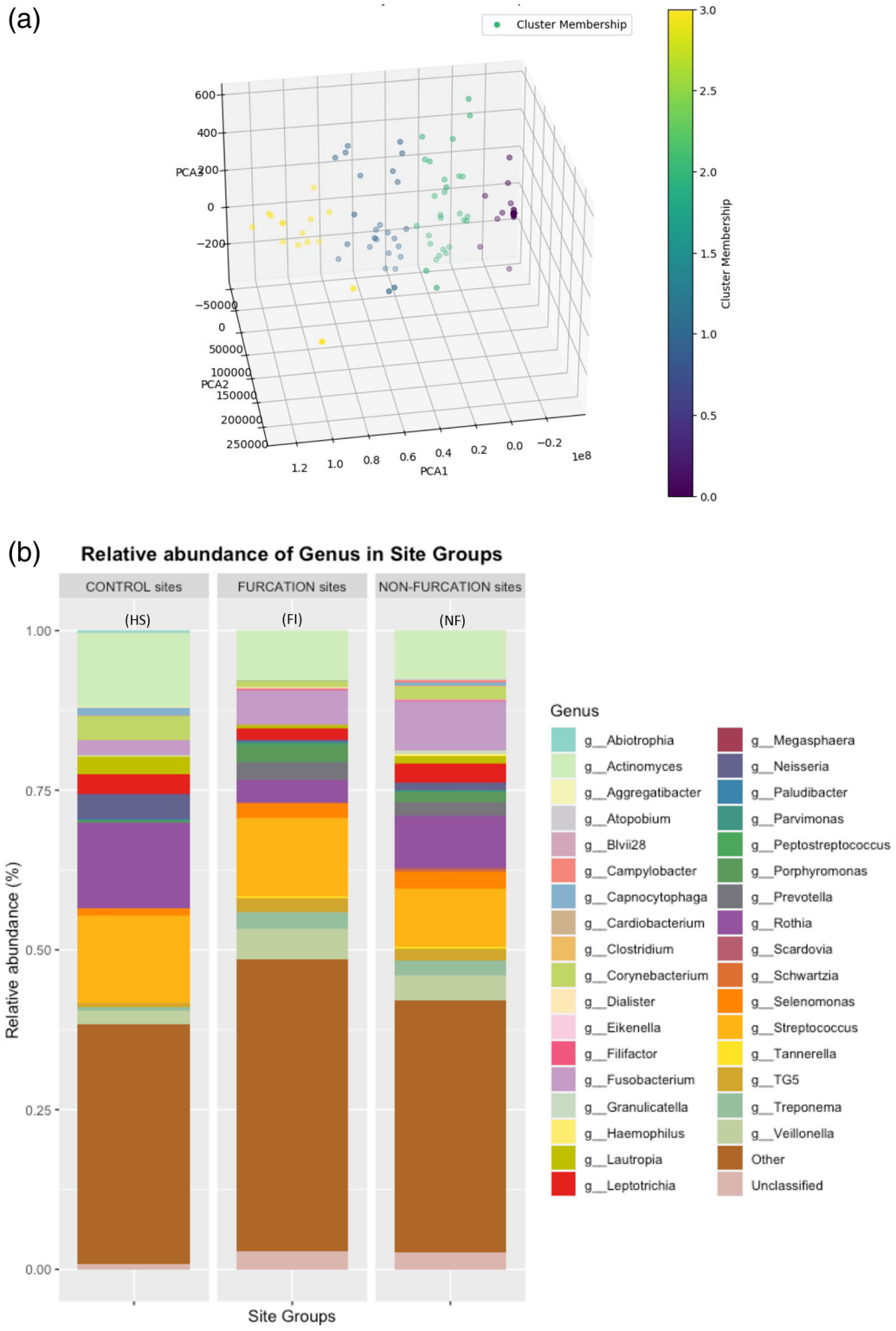

FIGURE 2 (a) Principal coordinates analysis for three-dimensional plotting, enabling visual discrimination of the four clusters. (b) Relative abundance of the top 34 bacterial genera identified in the study subjects grouped by furcation sites (FI), non-furcation (NF) and healthy sites (HS). The label 'Other' includes the taxa not included in the top 34 genera represented in the microbiome; the label 'unclassified' includes taxa not classified by the bioinformatic analysis.

IL-1α, IL-1β, IL-6, FAP-α, MMP-3, MMP-8, PDGF-AA, PDGF-BB, SOST, EGF, TIMP-1 and VEGF, with no significant difference for BMP-2, RANKL, INF-γ, IL-10, IL-17 and OPN. FI compared with NF showed a statistically significant increase in GCF levels of IL-6 ($p = .0001$), MMP-3 ($p = .003$), MMP-8 ($p = .008$), BMP-2 ($p = .008$), SOST ($p = .0001$), EGF ($p = .03$) and TIMP-1, ($p = .015$) (Table 2).

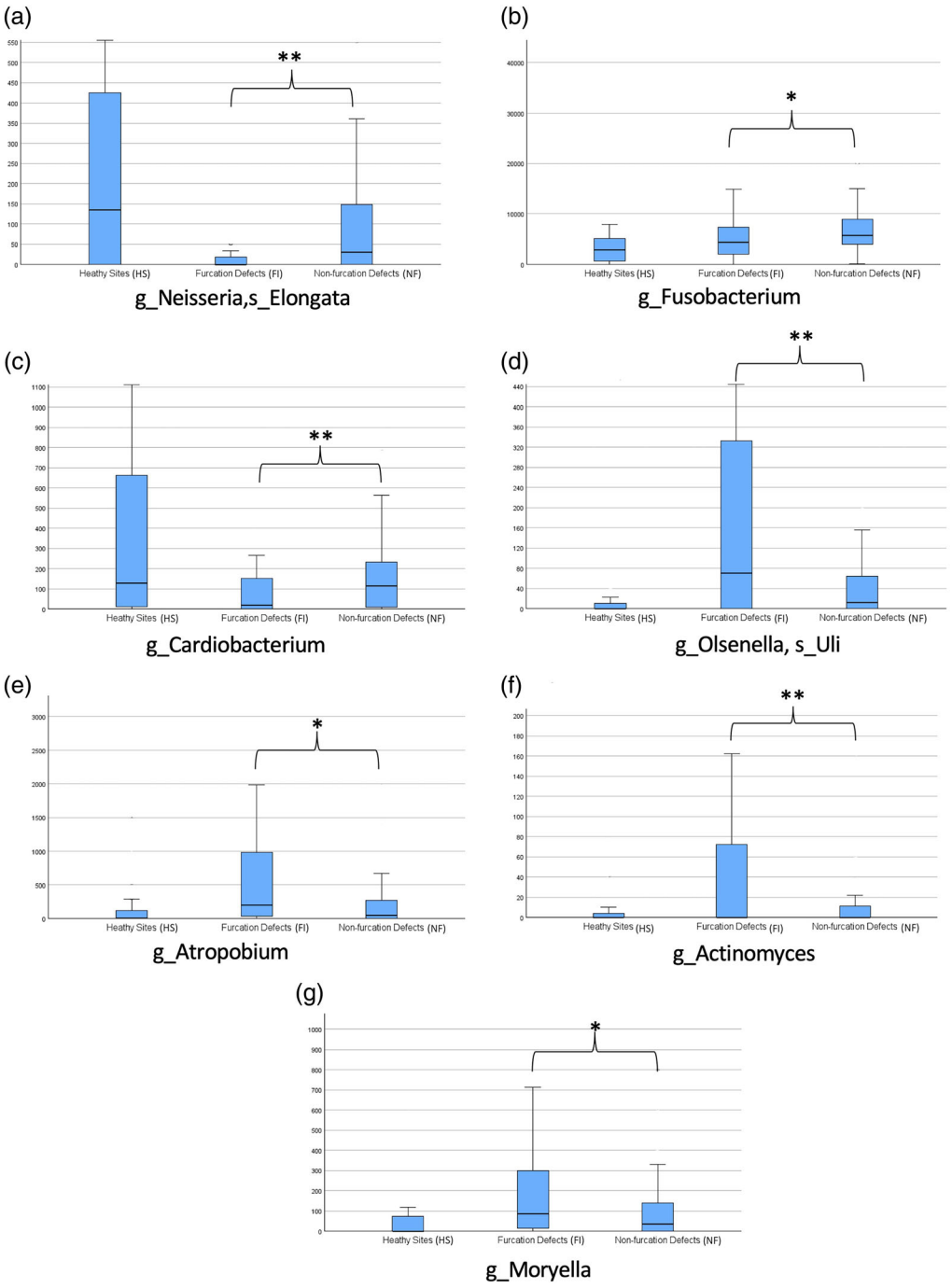

FIGURE 3 Relative abundance difference of the seven genera between furcation (FI), non-furcation (NF) and healthy site (HS). *p*-values: * indicates values below the significance level of .05, ** indicates values below the significance threshold of .001.

3.4 | Correlation of molecular biomarkers with subgingival microbiota

Figure 5 shows the Pearson correlation between molecular biomarkers and the 50 most represented taxa in FS, NF and HS. In general, a positive correlation (>.2) was detected between molecular biomarkers and taxa, including genera defined as 'red' and 'orange 'complex, and a negative correlation (<.2) with the taxa defined as 'green' and 'yellow' complex. Further results are included in SupMat4.

4 | DISCUSSION

Periodontal furcation defects are characterized by a unique anatomy, which facilitates plaque build-up and leads to progressive bone loss and a higher relative risk of tooth loss. However, little is known about the specific microbiological profile and molecular-driven inflammatory events responsible for this higher rate of tissue destruction. This is the first study to profile the furcation microbiome and its GCF milieu compared with NF and HS. While more microbial diversity and

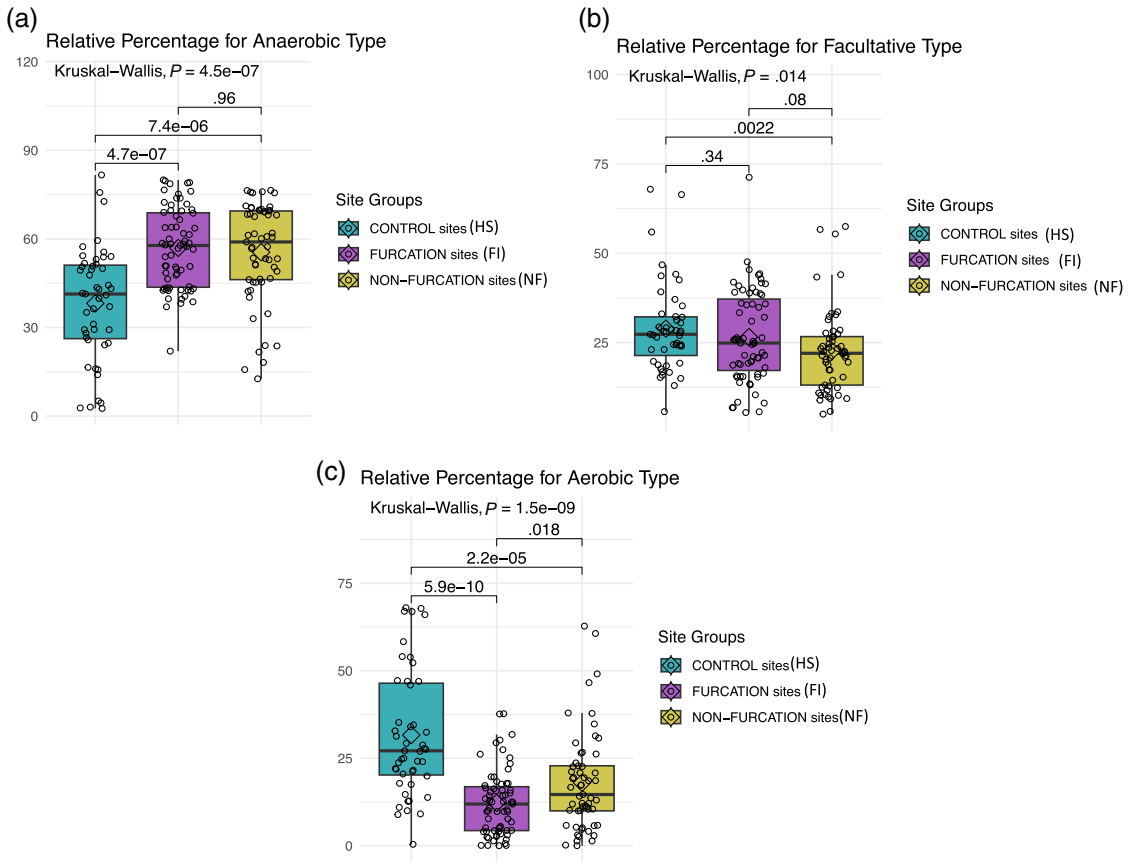

FIGURE 4 Relative percentage of aerobic, anaerobic and facultative taxa, grouped by furcation sites (FI), non-furcation (NF) and healthy sites (HS).

richness were detected in periodontal sites when compared with HS, the microbiome of FI contained a reduced aerobic component, suggesting that the complex anatomical configuration of furcation defects may play an important role in shaping the subgingival biofilm in patients with untreated periodontitis.

These findings are in agreement with a previous study reporting that FI showed richer and less aerobic counts of microorganisms when compared with non-molar sites, and this may be related to the difficulties in achieving complete debridement of furcation pockets (Loos et al., 1988). Furthermore, the same authors argued that their results may also reflect limitations of the plaque collection, phase-contrast microscopy and anaerobic culturing techniques used to conduct the analysis (Loos et al., 1988; Pihlstrom et al., 1985). Previous 16s rRNA analysis of FI comparing two surgical procedures concluded that the furcation microbiome appeared to be different from interproximal lesions, similar to the findings presented in this study where a less aerobic component and different genera were found between FI and NF. In line with previous data, richness and diversity in subgingival microbiome were increased in both FI and NF compared with HS, indicating that the incorporation of late colonizers into the subgingival biofilm increases the overall pathogenetic community as part of the dysbiosis (Arredondo et al., 2023; Griffen et al., 2012). Interestingly, the present study confirmed that periodontal pathogens may also be detected in HS in patients with periodontitis, which may be related to the intraoral translocation of periodontal pathogens from periodontal pockets to healthy sulcus with colonization of the diseased-free sites (Lourenço et al., 2014). Whether the increased percentage of pathogenic microorganism in HS will lead to dysbiosis, and consequently bone loss, is unknown (Lourenço et al., 2014). Accordingly, genera commonly associated with periodontitis were significantly more represented in both types of periodontal defects, while *Streptococcus*, *Rothia*, *Neisseria* and *Lautropia* were elevated in health, in line with previous reports and confirming the robustness of the microbial analysis reported here (Cai et al., 2021; Socransky et al., 2000). Interestingly, few genera such as *Olsenella*, *Atropobium*, *Moryella* and *Actinomyces* (Abusleme et al., 2013; Paster et al., 2001; Vielkind et al., 2015), previously associated with periodontitis, were more abundant in the furcation area compared with NF. However, the difference of few genera between FI and NF is not sufficient to comprehensively justify the complexity of mechanisms underlying the higher rate of progression and tooth loss observed in FI compared with other periodontal defects. It can be argued that the anatomical configuration of furcations could select a unique microbiological community; in fact, the heterogenous furcation anatomy could affect environment characteristics and determine microbial diversity (Queiroz et al., 2017).

To the authors' knowledge, this was the first study to apply an AI-based model to cluster the microbiological profile in individuals with periodontal defects and to evaluate the correlation between

TABLE 2 Gingival crevicular fluid cytokine marker concentrations (pg/mL) in diseased (furcation defects and non-furcation defects) and periodontally healthy sites.

	Healthy sites (HS)		Furcation sites (FI)		Non-furcation site (NF)		Difference NF-HS *p*-value	Difference FI-HS *p*-value	Difference NF-F *p*-value	Difference HS-disease (FI + NF) *p*-value
	N	Mean (SD)	*N*	Mean (SD)	*N*	Mean (SD)				
BMP-2	28	3.62 (1.1)	28	4.37 (1.12)	28	3.6 (1.28)	.951	.010*	.008**	.145
FAP-α	28	1.72 (4.12)	28	14.95 (32.6)	28	6.87 (10.67)	.002**	.0001***	.262	.0001***
IL-1α	28	201.01 (596.34)	28	504.22 (734.54)	28	484.04 (813.96)	.096	.0001***	.514	.0001***
IL-6	28	2.96 (4.05)	28	11.57 (6.69)	28	5.07 (5.64)	.0001***	.0001***	.0001***	.0001***
IL-17	28	0.74 (0.96)	28	0.76 (0.73)	28	0.85 (0.56)	.010*	.161	.238	.21
MMP-8	28	5273.06 (9605.83)	28	32158.12 (23160.67)	28	17244.08 (19684.88)	.005**	.0001***	.008**	.0001***
PDGF-AA	28	0.83 (1.51)	28	2.79 (5.66)	28	1.57 (1.48)	.003**	.0001***	.268	.0001***
SOST	28	6.53 (9.21)	28	21.72 (10.79)	28	8.98 (11.42)	.524	.0001***	.0001***	.001***
RANKL	28	7.29 (10.74)	28	5.65 (6.82)	28	6.36 (7.41)	.619	.712	.543	.523
EGF	28	6.92 (14.09)	28	12.72 (11.83)	28	9.09 (10.8)	.38	.0001***	.031*	.0001***
INF-γ	28	4.85 (4.48)	28	6.14 (4.77)	28	5.13 (3.85)	.314	.015*	.153	.47
IL-1β	28	85.57 (144.86)	28	336.52 (343.76)	28	218.01 (280.29)	.005**	.0001***	.071	.0001***
IL-10	28	5.41 (12.79)	28	2.98 (2.96)	28	4.12 (8.81)	.113	.01*	.322	.731
MMP-3	28	14.84 (17.41)	28	91.80 (90.01)	28	61.93 (118.89)	.026**	.0001***	.003**	.0001***
OPN	28	615.01 (918.36)	28	632.18 (498.39)	28	652.82 (579.62)	.631	.921	.756	.031
PDGF-BB	28	0.84 (0.62)	28	0.89 (0.39)	28	1.19 (0.58)	.0001***	.069	.743	.002**
TIMP-1	28	424.77 (309.51)	28	818.24 (707.51)	28	860.85 (661.62)	.013*	.005**	.015**	.002**
VEGF	28	15.93 (13.56)	28	50.84 (36.45)	28	31.07 (20.78)	.003**	.0001***	.067	.0001***

Note: Data are reported as means (standard deviations). * indicates statistical significant differences between sites $p < .05$; ** $p < .001$;*** $p < .0001$.

Abbreviations: BMP-2, Bone morphogenic protein-2; EGF, epidermal growth factor; FAPα, fibroblast activation protein alpha; IFN-γ, interferon-gamma; IL-10, interleukin-10; IL-17, interleukin-17; IL-1α, interleukin-1α; IL-1β, interleukin 1-β; IL-6, interleukin-6; MMP-3, matrix metalloproteinase-3; MMP-8, matrix metalloproteinase-8; OPN, osteopontin; PDGF-AA, platelet-derived growth factor-AA; PDGF-BB, platelet-derived growth factor-BB; RANKL, receptor activator of nuclear factor kappa-B; SOST, sclerostin; TIMP-1, tissue inhibitor metalloproteinase-1; VEGF, vascular endothelial growth factor.

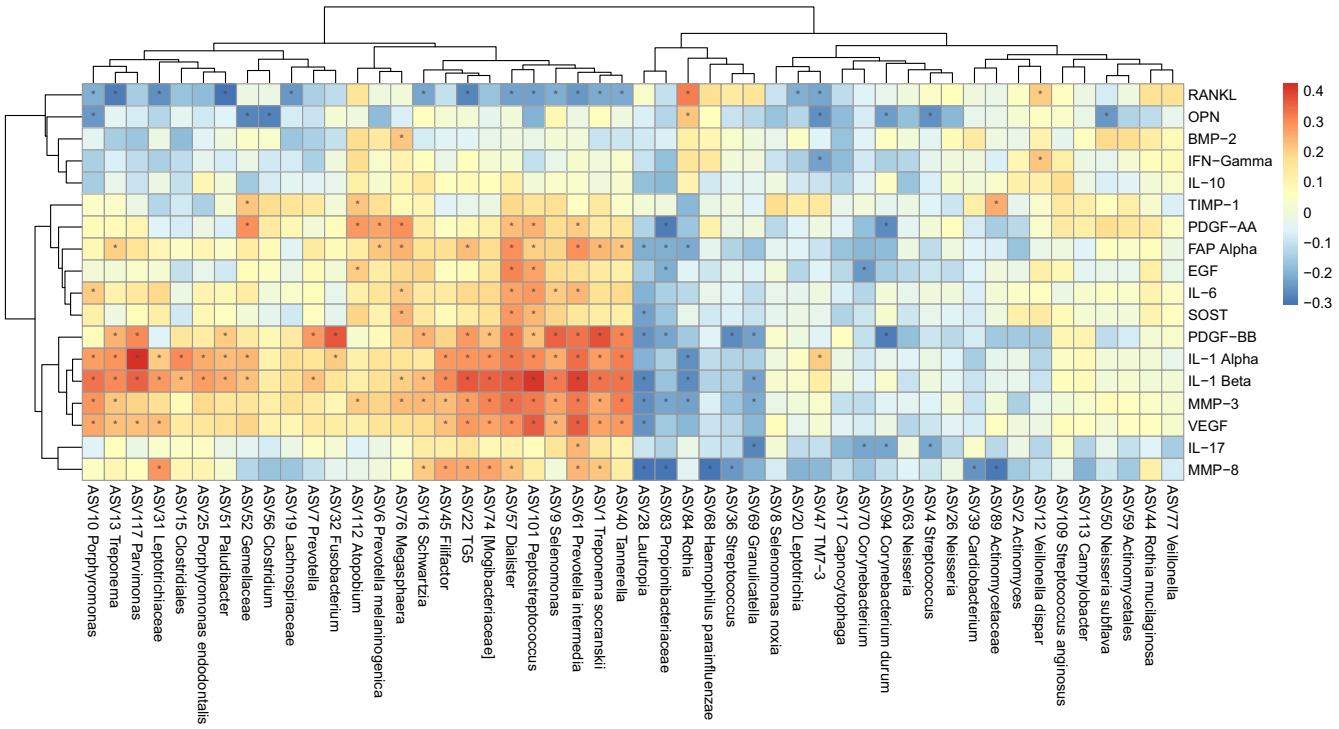

FIGURE 5 Heat map of the correlation between 18 biomarkers and bacterial genera detected in furcation, non-furcation sites and healthy sites.

these microbial profiles and defect morphology. The AI-based model was able to process large volumes of these microbiome data, identifying patterns that were missed by traditional methods, in particular the k-means clustering was able to identify patterns in microbiome data without the need for labelled training data, which allowed for exploration and discovery of novel microbial interactions. The model was able to successfully distinguish four different clusters from 0 ('more dysbiotic' taxa), to 3 ('less dysbiotic' taxa). Surprisingly, a trend to distinguish diseased and HS was observed just using microbiological similarities of the unlabelled data provided. Specifically, a site showing cluster 0 was associated with the microbiological profile of a periodontal defect in 80% of cases. Interestingly, cluster 0 was not only detected in periodontal defects but also in HS, suggesting that sites with no clinical and radiological evidence of disease may host the same pathogenic cluster as periodontal defects (Lourenço et al., 2014). Furthermore, while FI and NF were more predominant in cluster 0, HS showed an almost homogenous distribution among the four clusters, emphasizing that the absence of clinical signs of disease should not exclude the presence of a dysbiotic environment.

Another interesting finding of this study is the apparent presence of unique molecular features in the GCF of FI. Interestingly, although the GCF volume was slightly higher in furcation defects, no difference was detected when compared with the matched-periodontal defects, suggesting that the inflammatory process hosted in FI did not affect the quantity but rather the contents of the GCF. This result may be explained by a previous study that found how the GCF volume reflects the overall level of inflammation rather than a site-specific effect (Barros et al., 2016). Furthermore, a positive Pearson correlation was detected between molecular biomarkers and genera well known as periodontal pathogens, while a negative association was detected with genera usually associated with periodontal health. These results indicated that a linear correlation exists between certain microbial genera and biological factors, indicating how certain genera may thrive in environments determined by specific host factors. However, potential cofounders related to putative undetected microbial interactions, host–microbiome interactions, sample collection and processing methods should be considered in the interpretation of the previous findings. Interestingly, an elevation in several molecular biomarkers was detected in FI, such as IL-6 significantly associated with deep pocket depths and severe periodontal inflammation (Silva-Boghossian et al., 2013), or MMP-3 and MMP-8, which are associated with degradation of connective tissue collagen and alveolar bone (Barros et al., 2016). Unfortunately, no previous data are available to validate these findings. However, the anatomical features of FI include a variety of deposits of cellular cementum, islands, droplets, projections of enamel and several concavities observed in variable combinations (Roussa, 1998; Svärdström & Wennström, 1988). This complex morphology has a significant impact on plaque accumulation by favouring the retention of bacterial deposits (Roussa, 1998) with potentially more heterogenous microbiome and a less aerobic environment (Loos et al., 1988). In addition, it can be also speculated that the increased level of inflammatory, tissue degradation and repair biomarkers detected in the GCF may respond to the complex microbial challenge and represent indirect evidence of how host–microbial

interactions in periodontal defects may differ from other types of periodontal defects.

The strengths of this study are its novelty due to a comprehensive microbial and molecular analysis of furcation defects and the fact that clinical examinations, sample collection and DNA extraction were performed by a single operator. In terms of generalizability of our findings to other populations, these results should be validated on different cohorts, taking into consideration how different countries may have an effect on the microbiota (Arredondo et al., 2023). The genus-level analysis of microbiome might not fully capture how finer variations within species may differ among samples or experimental conditions, representing the main limitation of this study. The second limitation is the cross-sectional design of the study, which is only able to capture a snapshot of microbiological features at one point in time. Further limitations are related to potential statistical bias, such as the overly conservative Bonferroni correction, that may increase the type II error and the Pearson correlation that is unable to identify a non-linear correlation between genera and biological markers. Future research should focus on the analysis of furcation microbiome in different populations after debridement and surgical procedures to better understand the very complex and sophisticated mechanisms underlying the higher-rate attachment loss progression in furcation defects.

In conclusion, the present study showed that significant lower aerobic levels combined with an increased level of host mediators may represent specific signatures of the periodontal aetiopathogenesis in the furcation area, implying that the anatomical complexity of furcation may potentially interact with a specific microbial profile to drive a unique molecular response.

AUTHOR CONTRIBUTIONS

Study conception and design: Pasquale Santamaria and Luigi Nibali. *Data collection*: Pasquale Santamaria. *Analysis and interpretation of data*: Pasquale Santamaria, Yi Jin, Saeed Shoaie, David Spratt, Giuseppe Troiano and Luigi Nibali. *Drafting the manuscript*: Pasquale Santamaria and Luigi Nibali. *Review of the manuscript*: Pasquale Santamaria, Yi Jin, Giuseppe Troiano, Luigi Nibali and Mandeep Ghuman.

CONFLICT OF INTEREST STATEMENT

The authors declare no conflicts of interest.

DATA AVAILABILITY STATEMENT

The data that support the findings of this study are available from the corresponding author upon reasonable request.

ORCID

Pasquale Santamaria https://orcid.org/0000-0003-4102-1759
Giuseppe Troiano https://orcid.org/0000-0001-5647-4414
Luigi Nibali https://orcid.org/0000-0002-7750-5010

REFERENCES

Abusleme, L., Dupuy, A. K., Dutzan, N., Silva, N., Burleson, J. A., Strausbaugh, L. D., Gamonal, J., & Diaz, P. I. (2013). The subgingival microbiome in health and periodontitis and its relationship with community biomass and inflammation. *The ISME Journal*, *7*(5), 1016–1025. https://doi.org/10.1038/ismej.2012.174

Al-Shammari, K. F., Kazor, C. E., & Wang, H. L. (2001). Molar root anatomy and management of furcation defects. *Journal of Clinical Periodontology*, *28*(8), 730–740. https://doi.org/10.1034/j.1600-051x.2001.280803.x

Arredondo, A., Àlvarez, G., Isabal, S., Teughels, W., Laleman, I., Contreras, M. J., Isbej, L., Huapaya, E., Mendoza, G., Mor, C., Nart, J., Blanc, V., & León, R. (2023). Comparative 16S rRNA gene sequencing study of subgingival microbiota of healthy subjects and patients with periodontitis from four different countries. *Journal of Clinical Periodontology*, *50*(9), 1176–1187. https://doi.org/10.1111/jcpe.13827

Barros, S. P., Williams, R., Offenbacher, S., & Morelli, T. (2016). Gingival crevicular fluid as a source of biomarkers for periodontitis. *Periodontology 2000*, *70*(1), 53–64. https://doi.org/10.1111/prd.12107

Cai, Z., Lin, S., Hu, S., & Zhao, L. (2021). Structure and function of oral microbial community in periodontitis based on integrated data. *Frontiers in Cellular and Infection Microbiology*, *11*, 663756. https://doi.org/10.3389/fcimb.2021.663756

Gill, T., Bahal, P., & Nibali, L. (2022). Furcation-involved molar teeth - part 1: Prevalence, classification and assessment. *British Dental Journal*, *233*(10), 847–852. https://doi.org/10.1038/s41415-022-5202-x

Glickman, I. (1950). Bifurcation involvement in periodontal disease. *Journal of the American Dental Association (1939)*, *40*(5), 528–538. https://doi.org/10.14219/jada.archive.1950.0087

Griffen, A. L., Beall, C. J., Campbell, J. H., Firestone, N. D., Kumar, P. S., Yang, Z. K., Podar, M., & Leys, E. J. (2012). Distinct and complex bacterial profiles in human periodontitis and health revealed by 16S pyrosequencing. *The ISME Journal*, *6*(6), 1176–1185. https://doi.org/10.1038/ismej.2011.191

Hamp, S. E., Nyman, S., & Lindhe, J. (1975). Periodontal treatment of multirooted teeth. Results after 5 years. *Journal of Clinical Periodontology*, *2*(3), 126–135. https://doi.org/10.1111/j.1600-051x.1975.tb01734.x

Koidou, V. P., Hagi-Pavli, E., Cross, S., Nibali, L., & Donos, N. (2022). Molecular profiling of intrabony defects' gingival crevicular fluid. *Journal of Periodontal Research*, *57*(1), 152–161. https://doi.org/10.1111/jre.12948

Loos, B., Claffey, N., & Egelberg, J. (1988). Clinical and microbiological effects of root debridement in periodontal furcation pockets. *Journal of Clinical Periodontology*, *15*(7), 453–463. https://doi.org/10.1111/j.1600-051x.1988.tb01600.x

Lourenço, T. G. B., Heller, D., Silva-Boghossian, C. M., Cotton, S. L., Paster, B. J., & Colombo, A. P. V. (2014). Microbial signature profiles of periodontally healthy and diseased patients. *Journal of Clinical Periodontology*, *41*(11), 1027–1036. https://doi.org/10.1111/jcpe.12302

Nibali, L., Krajewski, A., Donos, N., Völzke, H., Pink, C., Kocher, T., & Holtfreter, B. (2017). The effect of furcation involvement on tooth loss in a population without regular periodontal therapy. *Journal of Clinical Periodontology*, *44*(8), 813–821. https://doi.org/10.1111/jcpe.12756

Paster, B. J., Boches, S. K., Galvin, J. L., Ericson, R. E., Lau, C. N., Levanos, V. A., Sahasrabudhe, A., & Dewhirst, F. E. (2001). Bacterial diversity in human subgingival plaque. *Journal of Bacteriology*, *183*(12), 3770–3783. https://doi.org/10.1128/JB.183.12.3770-3783.2001

Pellegrini, G., Rasperini, G., Pagni, G., Giannobile, W. V., Milani, S., Musto, F., & Dellavia, C. (2017). Local wound healing biomarkers for real-time assessment of periodontal regeneration: Pilot study. *Journal of Periodontal Research*, *52*(3), 388–396. https://doi.org/10.1111/jre.12403

Pihlstrom, B. L., Liljemark, W. F., Schaffer, E. M., Wolff, L. F., Smith, J. A., & Bandt, C. L. (1985). The relationship of probing depth and total microscopic counts to differential subgingival plaque morphology. *Journal of Periodontal Research*, *20*(1), 106–112. https://doi.org/10.1111/j.1600-0765.1985.tb00417.x

Queiroz, L. A., Casarin, R. C. V., Dabdoub, S. M., Tatakis, D. N., Sallum, E. A., & Kumar, P. S. (2017). Furcation therapy with enamel matrix derivative: Effects on the subgingival microbiome. *Journal of Periodontology*, *88*(7), 617–625. https://doi.org/10.1902/jop.2017.160542

Roussa, E. (1998). Anatomic characteristics of the furcation and root surfaces of molar teeth and their significance in the clinical management of marginal periodontitis. *Clinical Anatomy*, *11*(3), 177–186. https://doi.org/10.1002/(SICI)1098-2353(1998)11:3<177::AID-CA5>3.0.CO;2-Q

Santamaria, P., Sari, A., & Nibali, L. (2023). Molecular profiling of gingival crevicular fluid fails to distinguish between infrabony and suprabony periodontal defects. *Journal of Clinical Periodontology*, *50*(10), 1315–1325. https://doi.org/10.1111/jcpe.13849

Seidel, C. L., Gerlach, R. G., Wiedemann, P., Weider, M., Rodrian, G., Hader, M., Frey, B., Gaipl, U. S., Bozec, A., Cieplik, F., Kirschneck, C., Bogdan, C., & Gölz, L. (2020). Defining metaniches in the Oral cavity according to their microbial composition and cytokine profile. *International Journal of Molecular Sciences*, *21*(21), 21. https://doi.org/10.3390/ijms21218218

Silva-Boghossian, C. M., Colombo, A. P. V., Tanaka, M., Rayo, C., Xiao, Y., & Siqueira, W. L. (2013). Quantitative proteomic analysis of gingival crevicular fluid in different periodontal conditions. *PLoS One*, *8*(10), e75898. https://doi.org/10.1371/journal.pone.0075898

Socransky, S. S., Haffajee, A. D., Smith, C., & Duff, G. W. (2000). Microbiological parameters associated with IL-1 gene polymorphisms in periodontitis patients. *Journal of Clinical Periodontology*, *27*(11), 810–818. https://doi.org/10.1034/j.1600-051x.2000.027011810.x

Svärdström, G., & Wennström, J. L. (1988). Furcation topography of the maxillary and mandibular first molars. *Journal of Clinical Periodontology*, *15*(5), 271–275. https://doi.org/10.1111/j.1600-051x.1988.tb01583.x

Tarnow, D., & Fletcher, P. (1984). Classification of the vertical component of furcation involvement. *Journal of Periodontology*, *55*(5), 283–284. https://doi.org/10.1902/jop.1984.55.5.283

Tonetti, M. S., Greenwell, H., & Kornman, K. S. (2018). Staging and grading of periodontitis: Framework and proposal of a new classification and case definition. *Journal of Periodontology*, *89*(Suppl 1), S159–S172. https://doi.org/10.1002/JPER.18-0006

Trullenque-Eriksson, A., Tomasi, C., Petzold, M., Berglundh, T., & Derks, J. (2023). Furcation involvement and tooth loss: A registry-based retrospective cohort study. *Journal of Clinical Periodontology*, *50*(3), 339–347. https://doi.org/10.1111/jcpe.13754

Vielkind, P., Jentsch, H., Eschrich, K., Rodloff, A. C., & Stingu, C.-S. (2015). Prevalence of *Actinomyces* spp. in patients with chronic periodontitis. *International Journal of Medical Microbiology*, *305*(7), 682–688. https://doi.org/10.1016/j.ijmm.2015.08.018

SUPPORTING INFORMATION

Additional supporting information can be found online in the Supporting Information section at the end of this article.

How to cite this article: Santamaria, P., Jin, Y., Ghuman, M., Shoaie, S., Spratt, D., Troiano, G., & Nibali, L. (2024). Microbiological and molecular profile of furcation defects in a population with untreated periodontitis. *Journal of Clinical Periodontology*, 1–12. https://doi.org/10.1111/jcpe.14034